

Microscopic Heterogeneity in a Bowlic Columnar Mesophase As Probed with Fluorescence Depolarization Measurements

Alberto Arcioni, Riccardo Tarroni, and Claudio Zannoni*

Dipartimento di Chimica Fisica e Inorganica, Università, Viale Risorgimento 4, 40136 Bologna, Italy

Enrico Dalcanale

Dipartimento di Chimica Organica e Industriale, Università, Viale delle Scienze, 43100 Parma, Italy

Annick Du vosel†

Istituto G. Donegani, Via Fauser 4, 28100 Novara, Italy

Received: April 3, 1995; In Final Form: August 1, 1995[⊗]

The time-dependent fluorescence depolarization decays of the fluorescent probe 1,6-diphenyl-1,3,5-hexatriene (DPH) in the ordered and isotropic phase of a columnar liquid crystal formed by bowl-shaped metacyclophane cores symmetrically substituted by twelve alkanoyloxy chains have been recorded at various temperatures and analyzed using the global target approach. The measurements in the mesophase can be successfully analyzed only assuming a microscopic inhomogeneity of the columnar phase, with the probe partitioned between two environments, i.e. polar cores and apolar aliphatic chains, showing very different ordering and dynamical characteristics. This behavior becomes evident only when all the fluorescence intensities, corresponding to different parallel and perpendicular orientations of the excitation and observation polarizers, are analyzed simultaneously. The picture emerging from the analysis supports other recent findings on this class of columnar systems.

1. Introduction

Columnar mesophases both with discotic and bowlic cores are assuming more and more importance.¹ Recently a new class of mesogenic molecules, characterized by a bowl-shaped central core surrounded by twelve sufficiently long acyclic chains, has been synthesized^{2,3} and studied by various techniques.⁴⁻⁶ The general structure of these mesogens is shown in Figure 1, where the R groups are acyclic substituents with the general formula $R = \text{COC}_n\text{H}_{2n+1}$ and $R_1 = \text{CH}_3$. The compounds with $n = 12, 13, 15$ and 17 show a hexagonal columnar mesophase with D_{6h} symmetry;⁵ i.e., there is no positional correlation between molecules stacked in different columns. Due to this stacking, one can identify two different regions in the mesophase: a core and an aliphatic chain microenvironment, which have in principle rather different characteristics.

Here we wish to investigate the behavior of a fluorescent solute dissolved in one of these bowlic phases. Our aim is to see if the probe experiences an homogeneous or inhomogeneous environment and how its order and dynamics change with temperature and particularly on going from the ordered to the isotropic phase. The problem is of interest in its own right as a means of characterizing columnar mesophases but can also be of practical interest, since the detailed behavior of dissolved dyes needs to be known in view of potential applications in electro-optic devices.⁷ Here we have studied the compound with $n = 13$, which exhibits the largest mesophase interval of the series, by means of the fluorescence polarization technique.^{8,9}

2. Experimental Section

The mesogenic compound was synthesized following a previously published procedure.³ 1,6-Diphenyl-1,3,5-hexatriene

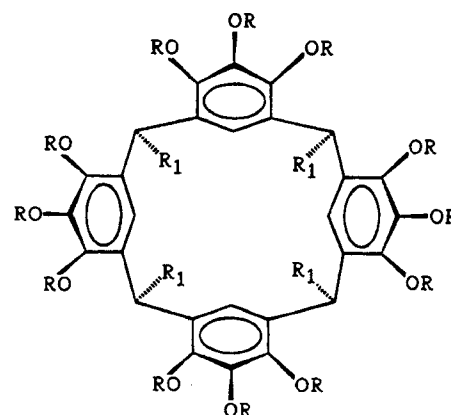


Figure 1. Structural representation of the bowl-shaped mesogen molecule. Here $R = \text{COC}_{13}\text{H}_{27}$ and $R_1 = \text{CH}_3$.

(DPH) and dichloromethane (HPLC grade) were obtained from Aldrich and used as supplied.

The fluorescent probe was incorporated into the liquid crystal by dissolving both in CH_2Cl_2 and then evaporating the solvent under vacuum. Thin macroscopically aligned samples were prepared by suitably spreading the doped columnar liquid crystal on a quartz slide, with a glass rod moving parallel to the surface. This operation was performed with the liquid crystal in the mesophase at a temperature close to the clearing point. Using this procedure, the resulting alignment was homogeneous, with the columns parallel to the quartz surface and to the shearing direction. The quality and reproducibility of the samples were checked by microscopic observation under crossed polarizers and proved to be good. Unfortunately such a good alignment was only possible for very thin samples ($< 10 \mu\text{m}$ of thickness), making it essential to use a rather high probe concentration (1×10^{-3} w/w), even though it is still low enough to avoid energy transfer depolarization.

* Author for correspondence

† Present address: Procos S.p.A., 28062 Cameri, Novara, Italy.

⊗ Abstract published in *Advance ACS Abstracts*, October 1, 1995.

The quartz cell was thermostated by a water circulation from a Lauda RCS 6-D thermostat equipped with a Lauda external controller R22 and a platinum resistance thermometer (Pt100 probe) located near the sample. The system ensured a temperature stability of 0.01 K over many hours. Single-photon measurements⁹ were performed on an apparatus described in a previous paper.¹⁰ DPH was excited at 358 nm and fluorescence observed at 460 nm with a transparency geometry. The excitation wavelength was selected by an Edinburgh Instruments model 121 grating monochromator and a band pass filter (Corning 5840) while the emission wavelength was selected by a similar monochromator in combination with a long-pass filter (Oriol 5217) with a cutoff wavelength of 420 nm. The excitation and emission polarizers were both Polaroid UV type HNP'B plastic. The flash lamp, Edinburgh Instruments model 199F, was filled with N₂ at a pressure of 1 atm and operated at a 25 kHz repetition rate with an electrode gap of 0.8 mm. The liquid crystal exhibits a columnar mesophase from 31 to 67 °C on heating.³ However all the measurements were performed above 48 °C for stability reasons.⁵ Due to the fact that the mechanical alignment is irreversibly lost above the clearing point, time-dependent fluorescence experiments were performed sampling seven temperatures on heating from 50 to 73 °C and allowing the sample to settle for 12 h before each measurement.

We considered the column axis to be along the Z laboratory direction, and we performed measurements of the fluorescence intensities $I_{ij}(t)$ with excitation and emission polarizers along directions e_i and e_j . In practice four fluorescence intensities, $I_{ZZ}(t)$, $I_{ZX}(t)$, $I_{XX}(t)$, and $I_{XZ}(t)$, were collected at each temperature, keeping the excitation polarization fixed and alternatively rotating the sample or the emission polarizer. Multiple photon detection (pile-up) problems⁹ were avoided, maintaining the start-stop count ratio below 2%. All the time decay curves had a channel width of 0.16 ns and a maximum height of 15 kcounts. The g_f correction factor⁹ accounting for the different sensitivity of the detection system to the vertical and horizontal polarizations was determined according to the procedure proposed in ref 11 and was found to be 0.87.

In Figure 2 we show the raw polarization anisotropies $r(t)$ (see section 3) resulting respectively from excitation parallel (curves a) and perpendicular (curves b) to the sample director at three different temperatures: two in the ordered phase (Figure 2A and B) and one in the isotropic phase (Figure 2C). The anisotropies show the expected long-time plateau corresponding to some kind of orientational order of the probe. The analysis of the curves will be tackled in the next sections.

3. Theory

In general, in a fluorescence polarization experiment, if fluorescent emission and molecular reorientation can be taken as independent processes, the observed intensity $I_{ij}(t)$ after an instantaneous excitation pulse can be expressed (see e.g. ref 12 for a more complete discussion) as

$$I_{ij}(t) = \langle |e_i \cdot \mu(0)|^2 |e_j \cdot \bar{\mu}(t)|^2 \rangle F(t) \quad (1)$$

where μ and $\bar{\mu}$ are the absorption and emission transition moments and $F(t)$ is the intrinsic fluorescence decay of the fluorophore. The brackets represent the average over all the relevant molecular motions up to time t . The observed fluorescence is then factorizable in two time-dependent terms related to the dynamics and the photophysics of the probe, respectively.

We treat DPH as a rigid rod with effective cylindrical symmetry around the long axis (the molecular z axis) and the

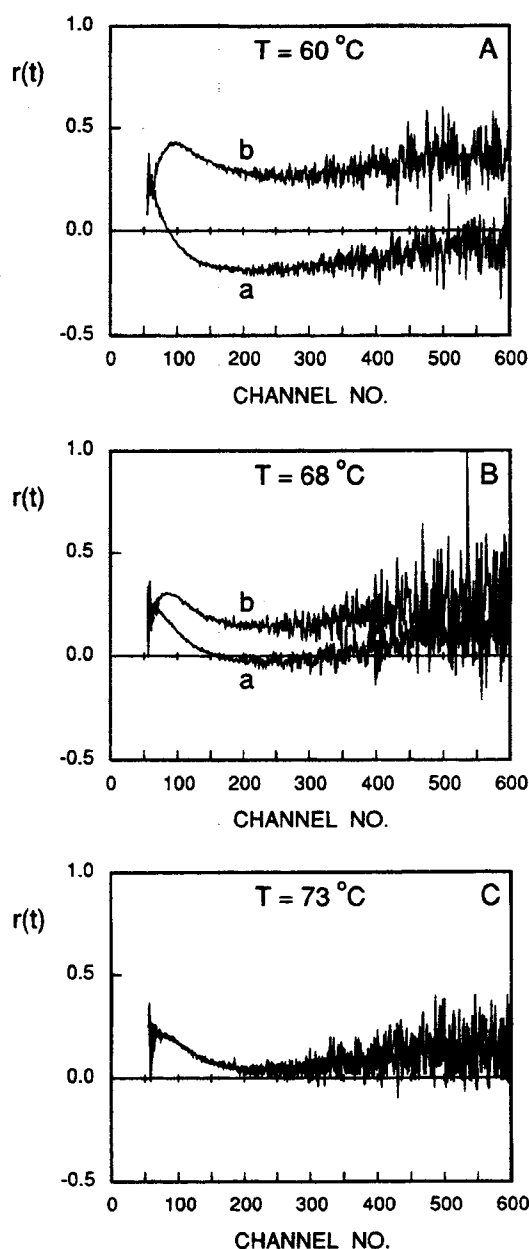


Figure 2. Experimental polarization ratios $r(t)$ obtained respectively in the columnar mesophase (A: $T = 60$ °C), close to the phase transition (B: $T = 68$ °C), and in the isotropic phase (C: $T = 73$ °C). The two curves in panels A and B correspond to the excitation polarizer set either parallel (a) or perpendicular (b) to the sample director. The time channel width is 0.16 ns.

same ordering in the ground and emitting state. These are only approximations¹³ but are nevertheless quite satisfactory when DPH is just employed to report about its environment and are in standard use.¹⁴ We also assume at first the mesophase to be homogeneous and to have both a microscopic and a macroscopic uniaxial symmetry with the director, here corresponding to the column axis, parallel to the laboratory Z axis. Thus the relevant equations for excitation parallel to the director are¹⁵

$$I_{ZZ}(t) = F(t) \left[\frac{1}{9} + \frac{6^{1/2}}{9} (A^{20} + \bar{A}^{20*}) \langle P_2 \rangle + \frac{2}{3} G_0(t) \right] \quad (2a)$$

$$I_{ZX}(t) = F(t) \left[\frac{1}{9} + \frac{6^{1/2}}{18} (2A^{20} - \bar{A}^{20*}) \langle P_2 \rangle - \frac{1}{3} G_0(t) \right] \quad (2b)$$

while those for excitation perpendicular to the director are

$$I_{XX}(t) = F(t) \left[\frac{1}{9} - \frac{6^{1/2}}{18} (A^{20} + \bar{A}^{20*}) \langle P_2 \rangle + \frac{1}{6} G_0(t) + \frac{1}{2} G_2(t) \right] \quad (3a)$$

$$I_{XZ}(t) = F(t) \left[\frac{1}{9} - \frac{6^{1/2}}{18} (A^{20} - 2\bar{A}^{20*}) \langle P_2 \rangle - \frac{1}{3} G_0(t) \right] \quad (3b)$$

Here $A^{2,n}$ and $\bar{A}^{2,n*}$ are spherical components of the absorption and emission dipole moment tensors $\mathbf{A} = \boldsymbol{\mu} \otimes \boldsymbol{\mu}$ and $\bar{\mathbf{A}} = \bar{\boldsymbol{\mu}} \otimes \bar{\boldsymbol{\mu}}$ while $\langle P_2 \rangle$ is the second-rank order parameter for the emitting probe. The functions $G_n(t)$, defined as

$$G_n(t) = \sum_{q=-2}^2 A^{2q} \bar{A}^{2q*} \langle D_{nq}^2(\omega_0) D_{nq}^{2*}(\omega_t) \rangle \quad (4)$$

contain information on the probe dynamics as a linear combination of the orientational correlation functions $\phi_{nq}(t) = \langle D_{nq}^2(\omega_0) D_{nq}^{2*}(\omega_t) \rangle^{16,17}$ of the second-rank Wigner rotation matrices $D_{mm'}^2(\omega_t)$ that give the molecular orientation at time t .

It is then possible to have two different polarization ratios $r(t)$, defined as $r(t) = [I_{||}(t) - I_{\perp}(t)]/[I_{||}(t) + 2I_{\perp}(t)]$, according to the direction of the excitation with respect to the director:

$$r_{ZZ,ZX}(t) = \frac{6^{1/2} \bar{A}^{20*} \langle P_2 \rangle + 6G_0(t)}{2(1 + 6^{1/2} A^{20} \langle P_2 \rangle)} \quad (5a)$$

$$r_{XX,XZ}(t) = \frac{-6^{1/2} \bar{A}^{20*} \langle P_2 \rangle + 3G_0(t) + 3G_2(t)}{2 - 6^{1/2} [A^{20} - \bar{A}^{20*}] \langle P_2 \rangle - 3G_0(t) + 3G_2(t)} \quad (5b)$$

Considering the long-time limit ($t \rightarrow \infty$) and transition moments parallel to the molecular z axis (i.e. $A^{20} = \bar{A}^{20*} = (2/3)^{1/2}$) one has

$$r_{ZZ,ZX}(\infty) = \langle P_2 \rangle \quad (6a)$$

$$r_{XX,XZ}(\infty) = -\langle P_2 \rangle / (1 + \langle P_2 \rangle) \quad (6b)$$

showing that the plateau for both geometries should depend on the local order. Thus if the probe tends to be perpendicular to the column axis, so that $\langle P_2 \rangle < 0$, we expect $r_{ZZ,ZX}(\infty) < 0$ and $r_{XX,XZ}(\infty) > 0$. From an inspection of Figure 2A we can see that the long-time behavior of the experimental $r(t)$ (curves a and b) essentially follows the corresponding eqs 6a and 6b.

For a probe with effective cylindrical symmetry like DPH the least biased orientational distribution function $f(\beta)$ which can be deduced from a fluorescence polarization experiment at a certain temperature T is, in the most favorable case,¹⁸⁻²⁰

$$f(\beta, T) = \exp[a_0(T) + a_2(T) P_2(\cos \beta) + a_4(T) P_4(\cos \beta)] \quad (7)$$

where $P_2(\cos \beta)$ and $P_4(\cos \beta)$ are the second- and fourth-rank Legendre polynomials and β is the angle between the molecular effective symmetry axis and the local director. In practice eq 7 corresponds to introducing an effective orientational anisotropic $P_2 - P_4$ potential for the probe

$$-U_{\text{probe}}(\beta, T)/k_B T = a_2(T) P_2(\cos \beta) + a_4(T) P_4(\cos \beta) \quad (8)$$

with k_B the Boltzmann constant, from which the order parameters can be evaluated as

$$\langle P_L \rangle = \frac{\int_0^\pi d\beta \sin \beta P_L(\cos \beta) \exp[-U_{\text{probe}}(\beta, T)/k_B T]}{\int_0^\pi d\beta \sin \beta \exp[-U_{\text{probe}}(\beta, T)/k_B T]}, \quad L = 2, 4 \quad (9)$$

The normalization condition of $f(\beta)$ determines a_0 , while a_2 and a_4 are temperature-dependent maximum entropy parameters which should give back the experimental $\langle P_2 \rangle$ and $\langle P_4 \rangle$ when introduced into eq 9. The same potential is inserted in a rotational diffusion equation^{12,15-17} for the probe dynamics, which is then solved to yield the correlation functions in eq 4. Thus the time evolution of the $r(t)$ in eq 5 depends both on the diffusion coefficients of the probe and on the local order it is subjected to. As a special case we talk of a pure- P_2 or a pure- P_4 potential if just the first or the second item of the expression in eq 8 is present.

The simple theory outlined here for a monodomain along the Z laboratory axis has actually been generalized^{20a,21a} to arbitrary transition moment orientations and to a variety of homogeneous systems, i.e. uniaxial monodomains at arbitrary tilt angles^{15,21a} and systems with a distribution of directors such as cylindrical phases²² and membrane vesicles.²³ Here we consider a system which is intrinsically more complex than those mentioned above. X-ray studies⁵ have shown that for this and similar compounds the molecules in the mesophase are stacked in columns with an high order parameter and with the apolar aliphatic chains radially disposed around the polar cores (here the core is intended to include also the ester group of the acyl chains (see Figure 1)). Inside the columns the molecules have been found to assume a 'boat' or 'flattened cone' conformation⁶ and to be paired in a head-to-head fashion.⁵ These two peculiarities make this type of mesophase particularly difficult to model, as the complex central cores can not *a priori* be assimilated to a 'disk' and, more important, microscopic homogeneity cannot be taken for granted. Moreover the molecular probe DPH has a length which approximately matches both that of the aliphatic chains in their elongated conformation and the diameter of the cores.

The theory can also be extended to the case of inhomogeneous systems where different environments exist and the observed fluorescence intensity can be considered as a sum of contributions from the various domains, as long as the time required by the probe to exchange between them is much longer than the observation time. Referring to our columnar system, such a slow exchange is consistent with previous deuterium NMR investigations,⁴ which moreover operate on a much slower time scale compared to fluorescence, and thus it seems natural to consider a two-site model with a 'core' and a 'chain' environment and the probe to be partitioned between the two domains. According to this physical picture the system is formally analogous to an homogeneous solvent containing two different fluorescent species which absorb and emit independently and have in general different order and dynamical characteristics. So the total observed intensity $I_{ij}(t)$ can be simply written as the sum of the time-dependent dynamical contribution of each probe weighted by its own fluorescence intensity, which in turn contains the respective populations

$$I_{ij}(t) = \langle |e_i \cdot \boldsymbol{\mu}(0)|^2 |e_j \cdot \bar{\boldsymbol{\mu}}(t)|^2 \rangle_1 F_1(t) + \langle |e_i \cdot \boldsymbol{\mu}(0)|^2 |e_j \cdot \bar{\boldsymbol{\mu}}(t)|^2 \rangle_2 F_2(t) \quad (10)$$

Here we assume the transition moments of the probe to be the same in the two environments, and the subscripts 1 and 2 label the two domains constituting the heterogeneous system or, equivalently, the two 'different' emitting molecular probes. Recently this kind of model has been used to account for

fluorescence anisotropy decays in vesicles,^{24,25} but, as far as we know, it has never been applied to thermotropic liquid crystals. In the next section we shall apply these various models to our data.

4. Data Analysis

In a series of papers^{10,20,21,26} we have shown that the quality of the results from the deconvolution of time-dependent fluorescence polarization data can be significantly improved using the global target analysis (GTA) approach, especially when the parameters involved in the fitting model are strongly correlated and/or affected by large statistical errors. The word 'global' means that all the available data are handled together in the same fitting procedure, while 'target' implies fitting some target parameters in a molecular model accounting for the decay of the fluorescence anisotropy, rather than using a simple sum of independent exponentials.

Data analysis was then performed in two steps. First we tried to set up a molecular model capable of fitting all four intensities collected at each temperature (we called this step individual target analysis (ITA)). Then we globalized the model to take into account the temperature dependence of the parameters involved in setting up the final global target fit. The experimental intensities have been analyzed using a deconvolution software package developed by our group,^{10,20,21,26} implementing both individual and global target analysis for all the adopted models with a Newton-Marquardt nonlinear least-squares fitting procedure.²⁷

As mentioned before it is difficult to think of this mesogenic system as a truly microscopically homogeneous one, but in the first instance, we treated it as such, introducing more complex models only if required to adequately describe the experimental data. Thus the first model we have tested is that, introduced in section 3, which assumes an homogeneous environment for the probe, with the system having both locally and macroscopically a uniaxial symmetry. This model has been successfully used in fluorescence polarization studies of probes dissolved in thermotropic calamitic (rod like) liquid crystals^{10,21b} and describes the order and dynamics of the fluorescent probe in terms of the following molecular parameters: (i) a_2 and a_4 , maximum entropy coefficients in the effective orienting potential which acts on the probe (see eq 8), (ii) D_{\perp} and D_{\parallel} , rotational diffusion coefficients of the probe, assumed to have an effective cylindrical symmetry, which describe respectively the tumbling motion of the molecular principal axis and the spinning around it (Notice that for a cylindrically symmetric probe D_{\parallel} does not contribute if at least one of the transition moments is parallel to the long axis.^{12,15}), and (iii) ϑ_{abs} and ϑ_{em} , angles giving the directions of the absorption and emission transition dipole moments with respect to the principal axis. For DPH ϑ_{abs} can be safely assumed to be zero so that the fitting parameters are limited to a_2 , a_4 , D_{\perp} , and ϑ_{em} for a $P_2 - P_4$ potential and to a_2 , D_{\perp} , and ϑ_{em} for the simpler pure- P_2 potential.

The above parameters are in general sufficient to describe the fluorescence anisotropy decay. For the intrinsic fluorescence decay a simple sum of two exponentials has been used. Additional fitting parameters, depending on the instrumental setup, are the overall scale factor, the time shift, that approximately accounts for the wavelength dependence of the detection system, and the fraction of excitation light reaching the photomultiplier in connection with each observed polarization component.⁹

The uniaxial homogeneous model, either using a pure- P_2 or a $P_2 - P_4$ potential, could not reasonably fit all four intensities at the same time (the final reduced sum of squared residuals

χ_r^2 ,²⁷ in the mesophase and using the $P_2 - P_4$ potential, ranges in fact from 3.030 to 1.543), while a good fit was obtained considering only the two intensities originating from the same polarization of excitation. In that case two different sets of molecular parameters were obtained. The value of $\langle P_2 \rangle$ was always negative for the temperatures within the mesophase, indicating that DPH tends to align perpendicularly to the columns. Moreover the intrinsic fluorescence decay of the probe was found to be markedly biexponential.

Next we tried to use a 'cylindrical' model,²² with a two-dimensional director distribution perpendicular to the column axis. In this case the system is assumed to have a macroscopically uniaxial symmetry, with the symmetry axis parallel to the columns, while microscopically the orientation of the local directors has a cylindrical symmetry, corresponding to the radial distribution of the chains around the cores. The number of fitting parameters is the same as in the uniaxial model, but in this case the value of $\langle P_2 \rangle$ is expected to be positive because DPH tends to align parallel to the alkyl chains (we recall that $\langle P_2 \rangle$ is always defined with respect to the local director). Even in this case the model did not readily reproduce all four intensities at the same time, but as for the uniaxial model, the two intensities related to the same polarization of excitation could be fitted and again two different set of parameters were obtained. Nevertheless the χ_r^2 values obtained in this case were systematically slightly higher than those in the previous series of analysis.

We also tested a novel model, that we called the 'tilt' model,²⁸ which allows a continuous variation of the orientation θ_r of the local director with respect to the macroscopic symmetry axis. The limiting cases of uniaxial and cylindrical models are obtained in correspondence with $\theta_r = 0^\circ$ and $\theta_r = 90^\circ$, respectively. When inserted into the fitting procedure, allowing the simultaneous optimization of θ_r with the other molecular parameters, the model showed a sort of bistability, tending to converge either to the results of the uniaxial model ($\theta_r \sim 0^\circ$) or to those of the cylindrical model ($\theta_r \sim 90^\circ$), depending on the choice of the starting parameters. This behavior was observed analyzing both two and four intensities at a time. So we concluded that this model too was not appropriate for describing the present columnar system even though it may be effective in dealing with truly tilted bowlic mesophases.^{29,30}

At this point we decided to go beyond the assumption of homogeneity for the system and to set up a model taking explicitly into account different environments for the probe. This choice is justified, as already mentioned, both by the structure of the columnar mesophase, in which the polar domains (the cores) are quite clearly separated from the nonpolar ones (the aliphatic chains), and by the strong biexponential character shown by the intrinsic fluorescence decay of DPH.

In fact it is known that DPH generally shows a single exponential decay at least in simple homogeneous and isotropic liquids, with a decay time tending to decrease as the polarity of the solvent increases.³¹ So it seems reasonable to associate the shorter lifetime of the biexponential decay to the fraction of DPH embedded between the cores of the mesogen and the longer one to the fraction dissolved into the aliphatic chains.

The two-site model eq 10 introduces for the second domain another set of fitting parameters. In practice only two (a_2 and D_{\perp}) or three (a_2 , a_4 , and D_{\perp}) new parameters are required, depending on the assumed anisotropic potential, either pure- P_2 or $P_2 - P_4$. When this model is applied to the simultaneous analysis of the four decays accumulated in a single experiment, the χ_r^2 value reduces to 1.1 ~ 1.2 for all the temperatures, indicating that the assumption on the probe partition is reason-

able. Indeed we applied two different two-site models, containing the same number of adjustable parameters, the first assuming a uniaxial distribution and a second one assuming a cylindrical distribution of directors, but the former gave a slightly but systematically lower χ_r^2 .

We then tried to globalize the fitting, handling all the experiments at all temperatures at the same time. We have shown elsewhere that this can increase the reliability of the results, by reducing the correlation between some of the fitting parameters.^{20,21,26} However the present case is complicated by the occurrence of a phase transition, which often involves a sharp change of some physical observable. The simplest globalization we can think of, and that is actually employed here, is one concerning only those parameters which show a smooth change across the phase transition. In practice only the two fluorescence decay times and the emission dipole moment angle ϑ_{em} were treated globally over the whole range of temperatures, assuming for the former a polynomial (parabolic) variation with temperature and considering the latter as temperature independent. The diffusion coefficients on the contrary were globalized only inside the mesophase, again using a parabolic expression.

The inclusion of the isotropic phase experiments in the adopted global fitting introduces some nontrivial complications. It is difficult to think of a heterogeneity in an isotropic phase, so that the two-site model eq 10 is not expected to be strictly applicable. On the other hand the photophysics of the probe can be influenced even by local polarity fluctuations. Thus for the measurements above the phase transition we used the simple one-site model eq 1, with a double-exponential fluorescence decay, but we forced each component to have a continuity relation (imposed by the selected parabolic globalization) with the corresponding single-exponential decay in the ordered phase.

Thus the globalization scheme can be summarized as follows: (i) The two-site model eq 10 was adopted within the mesophase while in the isotropic phase we used the one-site model eq 1. (ii) The simple pure- P_2 potential with uniaxial distribution was assumed in the mesophase for both environments. (iii) ϑ_{em} was kept the same for all the temperatures (one single adjustable parameter). (iv) $D_{\perp 1}$ and $D_{\perp 2}$ were globalized with a parabolic relation only within the mesophase (six temperatures), while a single $D_{\perp iso}$ was assumed in the isotropic phase (one temperature). (v) A single exponential decay time, τ_{F1} or τ_{F2} respectively, was associated with each site in the mesophase and globalized over all the temperatures with a parabolic expression. In the isotropic phase, on the other hand, a double-exponential fluorescence decay was assumed, with the individual decay times linked to those in the mesophase through the above-mentioned parabolic relation. (vi) All the remaining physical parameters, i.e. order parameters and fluorescence fractions (intensities), were fitted as local parameters for each temperature.

The results obtained from this fitting are summarized in Figure 3 and correspond to a global $\chi_r^2 = 1.580$. The χ_r^2 decreases a little if we remove the requirement of temperature independence for ϑ_{em} (which we found to be $\sim 22^\circ$), but this introduces large correlations between this parameter and one of the diffusion coefficients, leading to unphysical results. Similar correlations, which we were unable to remove, were observed using the $P_2 - P_4$ anisotropic potential, so that we resorted to using the simpler pure- P_2 potential.

The results shown agree nicely with recent findings about this class of liquid crystals⁴⁻⁶ and with the current knowledge of the fluorescence probe.³¹ The shortest decay time, coming from the fraction of DPH molecules experiencing a polar

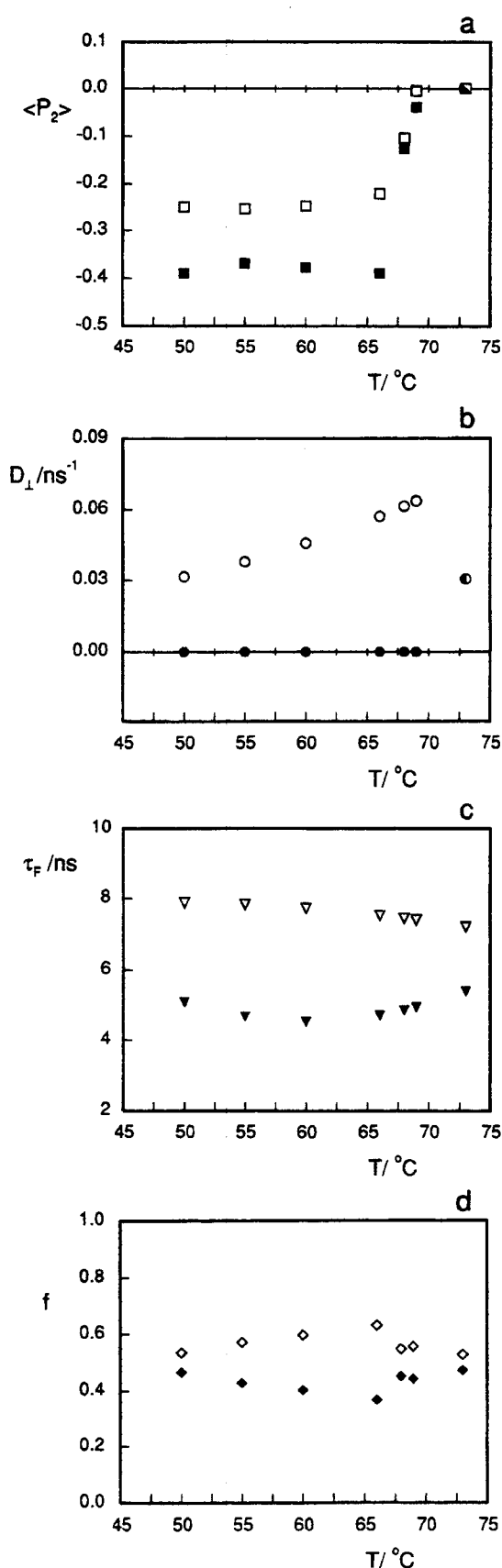


Figure 3. Results obtained from GTA using the two-site model with a pure- P_2 potential. In the mesophase range, full and empty symbols correspond to the parameters associated with the probe molecules respectively embedded in the column polar cores or dissolved into the aliphatic chains. The half-filled symbols in parts a and b refer to the value in the isotropic phase. Here we show the order parameters $\langle P_2 \rangle$ (a), the rotational diffusion coefficients D_{\perp} (b), the fluorescence decay times τ_F (c) (see text), and the normalized fluorescence intensities f (d) as a function of temperature T . The global χ_r^2 value is 1.580.

environment and hence attributable to the probe molecules embedded between the cores of the mesophase, is associated with a markedly higher order parameter and a very small diffusion coefficient. We point out that this basic immobility of DPH molecules on our experimental time scale is also consistent with a recent deuterium NMR study⁶ showing that the molecules of the mesogen do not rotate inside the columns.

The slower decay, on the other hand, is associated with a much lower order parameter and an higher, temperature-dependent, diffusion coefficient, and it can be attributed to the fraction of probe molecules dissolved into the aliphatic region formed by the apolar floppy side chains.

Deductions based on the fluorescence intensities are more difficult to make, because, as pointed out previously, these parameters include not only the fraction of probe molecules partitioned into the two environments but also their relative quantum yield. However, considering only the fractions in the mesophase, far away from the phase transition, we note a steady decrease of the fast decay component in favor of the slow one, consistent with the picture of a probe which is progressively found more frequently outside the mesophase-cores as the temperature increases.

5. Conclusions

In this work we have obtained and analyzed the time-dependent fluorescence polarization decays of the fluorescent probe DPH in the ordered and isotropic phase of a columnar liquid crystal formed by bowl-shaped molecules. A global target analysis shows that the polarization decays in the mesophase can be satisfactorily analyzed only assuming a microscopic inhomogeneity of the columnar phase, with the probe experiencing two different environments, i.e. the polar cores and the apolar aliphatic chains of the mesogenic molecules, with very different ordering and dynamical characteristics. In both environments the DPH probe tends to align perpendicular to the columns. In the central region the probe is highly ordered and reorients much more slowly than in the aliphatic chain region. In the isotropic phase the probe dynamics is consistent with the presence of only one average environment. We have also found that one could be misled in finding only one environment also in the mesophase by analyzing only a pair of measurements with a single polarizer excitation rather than a full set like here.

The presence of a macrocyclic core having a complex three-dimensional shape reduces or eliminates the exchange between the two regions, thus allowing the study of the localized behavior of such molecules in the columnar mesophase. In the emerging field of liquid crystalline compounds having complexation properties,^{32,33} fluorescence depolarization spectroscopy could be a useful handle in studying the behavior of chromophoric guests.

Acknowledgment. We are grateful to MURST, CNR, and the G. Donegani Institute for support. One of the authors (R.T.) is also particularly grateful to the G. Donegani Institute for a fellowship awarded to him during the initial stages of this work.

References and Notes

- (1) (a) Chandrasekhar, S. *Liq. Cryst.* **1993**, *14*, 3. (b) Malthête, J. *Adv. Mater.* **1994**, *4*, 315.
- (2) Cometti, G.; Dalcanale, E.; Du vosel, A.; Levelut, A. M. *J. Chem. Soc., Chem. Commun.* **1990**, 163.
- (3) Bonsignore, S.; Cometti, G.; Dalcanale, E.; Du vosel, A. *Liq. Cryst.* **1990**, *8*, 639.
- (4) Abis, L.; Arrighi, V.; Cometti, G.; Dalcanale, E.; Du vosel, A. *Liq. Cryst.* **1991**, *9*, 277.
- (5) Dalcanale, E.; Du vosel, A.; Levelut, A. M.; Malthête, J. *Liq. Cryst.* **1991**, *10*, 185.
- (6) Riccò, M.; Dalcanale, E. *J. Phys. Chem.* **1994**, *98*, 9002.
- (7) *Liquid Crystals, Applications and Uses*; Bahadur, B., Ed.; World Scientific: Singapore, 1990.
- (8) Michl, J.; Thulstrup, E. W. *Spectroscopy with Polarized Light*; VCH: New York, 1987.
- (9) O'Connor, D. V.; Phillips, D. *Time-Correlated Single Photon Counting*; Academic Press: London, 1984.
- (10) Arcioni, A.; Bertinelli, F.; Tarroni, R.; Zannoni, C. *Mol. Phys.* **1987**, *61*, 1161.
- (11) Mielenz, K. D.; Cehelnik, E. D.; McKenzie, R. L. *J. Chem. Phys.* **1976**, *64*, 370.
- (12) Zannoni, C.; Arcioni, A.; Cavatorta, P. *Chem. Phys. Lipids* **1983**, *32*, 179.
- (13) (a) Kintanar, A.; Kunvar, A. C.; Oldfield, E. *Biochemistry* **1986**, *25*, 6517. (b) Tarroni, R.; Zannoni, C. To be submitted for publication.
- (14) (a) Best, L.; John, E.; Jähnig, F. *Eur. Biophys. J.* **1987**, *15*, 87. (b) van Langen, H.; van Ginkel, G.; Levine, Y. K. *Liq. Cryst.* **1988**, *3*, 1301. (c) Lentz, B. R. *Chem. Phys. Lipids* **1989**, *50*, 171. (d) Wang, S.; Beechem, J. M.; Gratton, E.; Glaser, M. *Biochemistry* **1991**, *30*, 5565.
- (15) Zannoni, C. *Mol. Phys.* **1979**, *38*, 1813.
- (16) Nordio, P. L.; Segre, U. In *The Molecular Physics of Liquid Crystals*; Luckhurst, G. R., Gray, G. W., Eds.; Academic Press: London, 1979; Chapter 18, p 411.
- (17) Tarroni, R.; Zannoni, C. *J. Chem. Phys.* **1991**, *95*, 4550.
- (18) *The Maximum Entropy Formalism*; Levine, R. D., Tribus, M., Eds.; MIT Press: Cambridge, MA, 1979.
- (19) (a) Kooyman, R. P. H.; Levine, Y. K.; van der Meer, B. W. *Chem. Phys.* **1981**, *60*, 317. (b) Pottel, H.; Herreman, W.; van der Meer, B. W.; Ameloot, M. *Chem. Phys.* **1986**, *102*, 37.
- (20) (a) Arcioni, A.; Tarroni, R.; Zannoni, C. *Nuovo Cimento D* **1988**, *10*, 1409. (b) Arcioni, A.; Tarroni, R.; Zannoni, C. *Liq. Cryst.* **1989**, *6*, 63.
- (21) (a) Arcioni, A.; Tarroni, R.; Zannoni, C. In *Polarized Spectroscopy of Ordered Systems*; Samori, B., Thulstrup, E., Eds.; Kluwer: Dordrecht, 1988; p 421. (b) Arcioni, A.; Tarroni, R.; Zannoni, C. *Chem. Phys.* **1990**, *143*, 259.
- (22) Zannoni, C. *Chem. Phys. Lett.* **1984**, *110*, 325.
- (23) Zannoni, C. *Mol. Phys.* **1981**, *42*, 1303.
- (24) Ruggiero, A.; Hudson, B. *Biophys. J.* **1989**, *55*, 1125.
- (25) Ludescher, R. D.; Peting, L.; Hudson, S.; Hudson, B. *Biophys. Chem.* **1987**, *28*, 59.
- (26) (a) Arcioni, A.; Tarroni, R.; Zannoni, C. *J. Chem. Soc., Faraday Trans.* **1991**, *87*, 2457. (b) Arcioni, A.; Tarroni, R.; Zannoni, C. *J. Chem. Soc., Faraday Trans.* **1993**, *89*, 2815.
- (27) Bevington, P. R. *Data Reduction and Error Analysis for the Physical Sciences*; McGraw-Hill: New York, 1969.
- (28) Arcioni, A.; Tarroni, R.; Zannoni, C. To be submitted for publication.
- (29) Malthête, J.; Collet, A. *Nouv. J. Chim.* **1985**, *9*, 151.
- (30) Zimmermann, H.; Poupko, R.; Luz, Z.; Billard, J. Z. *Naturforsch.* **1985**, *40a*, 149.
- (31) Cehelnik, E. D.; Cundall, R. B.; Lockwood, J. R.; Palmer, T. F. *J. Phys. Chem.* **1975**, *79*, 1369.
- (32) (a) Xu, B.; Swager, T. M. *J. Am. Chem. Soc.* **1993**, *115*, 1159. (b) Xu, B.; Swager, T. M. *J. Am. Chem. Soc.* **1995**, *117*, 5011.
- (33) van Nunen, J. L. M.; Stevens, R. S. A.; Picken, S. J.; Nolte, R. J. *M. J. Am. Chem. Soc.* **1994**, *116*, 8825.

JP950933V